BULLETIN OF THE POLISH ACADEMY OF SCIENCES
TECHNICAL SCIENCES, Vol. 63, No. 3, 2015
DOI: 10.1515/bpasts-2015-0093

Eigenproblems in nanomechanics

A. MUC* and A. BANAŚ

Institute of Machine Design, Cracow University of Technology, 37 Jana Pawła II St., 31-864 Kraków, Poland

Abstract. The paper is semitutorial in nature to make it accessible to readers from a broad range of disciplines. Our particular focus is on cataloging the known problems in nanomechanics as eigenproblems. Physical insights obtained from both analytical results and numerical simulations of various researchers (including our own) are also discussed. The paper is organized in two broad sections. In the second section the attention is focused on the analysis of quantum dots. The analysis of electronic properties of strained semiconductor structures is reduced here to the solution of a linear boundary value problem (the classical Helmholtz wave equation). In Sec 3, we provide, intermixed with a literature review, details on various methods and issues in calculation free vibrations/loss of stability for carbon nanotubes. The effect of various parameters associated with the material anisotropy are addressed. Typically classical continuum mechanics, which is intrinsically size independent, is employed for calculations.

Key words: nanomechanics, carbon nanotubes, free vibrations, buckling, shells, beams.

Notation:

Latin symbols

A	–	the beam cross-sectional area,
A_{11}, A_{22}, A_{12}, A_{66}	–	the classical in-plane (membrane) stiffness for orthotropic laminates,
$D^{\gamma\eta}_{\alpha\beta}$	–	the matrices characterizing the deformation potential,
E	–	the Young modulus of the isotropic beam,
E_1, E_2, E_3	–	the Young moduli in the longitudinal (1), circumferential (2) and radial (3) directions of the shell/nanotube, respectively,
$E_{g,i}$	–	the band gap,
F	–	the stretching force in the beam,
G	–	the Kirchhoff modulus of the isotropic beam,
g_1^{kl}, g_2^{kl}, g_3^{kl}, g_4^{kl}, g_5^{kl}, g_6^{kl}	–	the Luttinger-Kohn parameters,
G_{12}, G_{13}, G_{23}	–	the Kirchhoff moduli of the shell/nanotube,
h	–	the equivalent shell thickness,
$H_{\alpha\beta}$	–	the Hamiltonian function coupling the energy of a charge carrier between energy bands α and β,
I	–	the beam area moment of inertia,
J	–	the beam rotary inertia,
$K_{\alpha\beta}$	–	the elastic stiffness matrix,
$K_{g\alpha\beta}$	–	the geometric stiffness matrix,
k,l	–	ranges over the four valence subbands referred to 1,2, respectively,
L	–	the shell/nanotube length,
l_i	–	the i-th beam length,
$L^{kl}_{\alpha\beta}$ $(\vec{\mathbf{r}})$	–	the matrices of four valence subbands,
M	–	the bending moment in the beam,
m	–	the free electron mass,
$m_\alpha(\lambda_E)$	–	the electron effective mass,
n, m	–	the circumferential and longitudinal wavenumbers, respectively,
P_i	–	the momentum matrix element,
q_α	–	the vector of the unknown mechanical response of the structure, i.e. the system of generalized displacements,
$\vec{\mathbf{r}}$	–	the position vector throughout the solid,
R	–	the cylindrical shell (carbon nanotube) radius,
V	–	the interatomic potential,
V_α	–	the confinement potential,
$V_{\alpha\beta}$	–	the effective potential field coupling energy bands α and β,
$V_{\alpha\beta band}$ $(\vec{\mathbf{r}})$	–	the total potential due to the energy misalignment of the valence band maxima,
$V_{\alpha\beta strain}$ $(\vec{\mathbf{r}})$	–	the potential due to the elastic strain $\varepsilon^{\gamma\eta}$ $(\vec{\mathbf{r}})$ that shifts and couples the energy bands,
x	–	the fractional content of alloying material.

Greek symbols

δ_i	–	the spin-orbit splitting in the valence band,
$\varepsilon^{\gamma\eta}$ $(\vec{\mathbf{r}})$	–	the elastic strain tensor,
θ_i	–	the i-th bond angle,
λ	–	the eigenvalue of the covariance matrix $\Sigma_{\alpha\beta}$,
$\lambda = \lambda_E$	–	the eigenvalue for quantum mechanics models (the energy of a particular quantum mechanical state),

*e-mail: olekmuc@mech.pk.edu.pl

$\lambda = \lambda_b$ – the eigenvalue for classical mechanics models (buckling or free vibrations),
$\nu_{12}, \nu_{13}, \nu_{23}$ – the Poisson ratios,
ρ – the shell/nanotube density,
$\Sigma_{\alpha\beta}$ – the covariance matrix,
$\Sigma_{\alpha\beta} = H_{\alpha\beta}$ – for quantum mechanics models,
$\Sigma_{\alpha\beta} = K_{\alpha\beta}$ – for continuum mechanics models,
φ_α – the eigenvector of the covariance matrix $\Sigma_{\alpha\beta}$,
$\varphi_\alpha = \psi_\alpha$ – for quantum mechanics models,
$\varphi_\alpha = q_\alpha$ – for continuum mechanics models,
ψ_α – the quantum mechanical wave function associated with energy band β,
ω – the angular velocity,
Ω – the space occupied by the semiconductor,
h – the reduced Planck constant.

Chemical elements

As – aresnic,
Ga – gallium,
In – indium.

1. Introduction

The analysis of the dynamical/acoustic behavior of structures, vehicles, or molecules in nanomechanics needs the numerical solution of linear or nonlinear eigenvalue problems (see e.g. [1–3] for a mathematical introduction). Eigenvalue problems arise in a wide variety of science and engineering applications, such as the dynamic analysis of mechanical systems (where the eigenvalues represent vibrational frequencies), the linear stability of flows in fluid mechanics or structures in solid mechanics (buckling problems), the stability analysis of time-delay systems, and electronic band structure calculations for photonic crystals. These problems present many mathematical challenges. For some there is a lack of underlying theory. For others numerical methods struggle to provide any accuracy or to solve very large problems in a reasonable time.

The trend towards extreme designs (such as in nano/micro-electromechanical (NEMS/MEMS) devices and superjumbo jets) means that these nonlinear eigenproblems are often poorly conditioned (hence difficult to solve accurately) while also having algebraic structure that should be exploited in a numerical method in order to ensure physical meaning of the computed results. The numerical methods are available in (commercial) software. We just buy bigger computers to handle the higher complexity? In general, we need better mathematical models, faster and more accurate numerical methods, robust implementations on modern computer architectures.

The mathematics is well-known and used in industrial engineering every day – see the description of classical approaches discussed in Refs [4, 5], such as e.g.: second order Arnoldi method, rational Krylov method, residual iteration method, Newton methods, Rayleigh quotient iterations, Jacobi-Davidson method, Arnoldi type methods.

In nanomechanics, an eigenproblem can be formulated as:

$$\Sigma_{\alpha\beta}\,\varphi_\alpha = \lambda\varphi_\alpha. \tag{1}$$

Depending on the assumed formulation, the form and the physical meaning of the symbols used in Eq. (1) is different.

Nanostructured materials have the potential to provide order-of-magnitude increases in stiffness-to-weight and strength-to-weight ratios relative to current materials used for structural engineering applications [6, 7] and for small-scale devices [8–10]. Since computing nanomechanical responses requires large systems, computationally affordable but less accurate classical atomistic treatments of the atomic scale are widely adopted and only multiscale classical atomistic-to-continuum bridging is achieved. The possible approaches can be divided into two groups:

A. Atomistic (quantum-mechanical or molecular dynamic) approach – determination and analysis of the most stable atomic structure equivalent to the minimization of many particle interaction energy,
B. Continuum approach – nanoobjects are represented as continuum (solid) structures.

However, because of the structure of interest extent over several micrometers or more in one direction, a full atomistic treatment is prohibitive. This situation demands new simulation methods and the vision is that nanoscale modeling will be achieved through a multiscale approach, where the continuum emerges from a precise, quantum mechanical description of the atomic scale. The first important step to achieve multiscale modeling is designing an atomistic scheme to compute the nanomechanical response with high accuracy. It may be done in different ways listed below:

- The Schrodinger equation – molecular orbital theory,
- Density functional theory,
- Tight-binding molecular dynamics,
- Classical potentials (Lennard-Jones, Tersoff-Brenner, ...).

An accurate atomistic description is highly desirable in computational nanomechanics. In order to deliver quantitative prediction, suited for the further engineering use, the accurate quantum-mechanical description of chemical bonding is needed. Furthermore, because the electronic subsystem is treated explicitly, electronic, optical or piezoelectric properties can be also derived. Unfortunately, the size range covered by quantum-mechanical methods (of a few hundred atoms) is the major impediment for using these methods in nanomechanics. This is despite the fact that the size limit increases rapidly due to parallel computing.

This work does not intend to advance nanomechanics by trying to enlarge the current computational limit for number of atoms that can be treated with quantum mechanical accuracy. Instead, the main idea is to demonstrate the mathematical and computational similarity arising in solving eigenvalue problems in nanomechanics to classical continuum mechanics. We intend to prove that in various problems nanomechanics is classical mechanics and the differences lies in the scale only

since meters (or millimeters) are replaced by nanometers only. Two types of nanostructures are discussed in details, i.e. quantum dots and carbon nanotubes, and, in this way different forms of eigenproblems (1).

2. Quantum Dots

In recent decades semiconductor quantum dots (QDs) have been the subject of many experimental, theoretical and technological investigations. The broader description of those problems is presented in Ref. [11]. QDs are tiny dimensionally confined (typically semiconductor) objects where quantum effects become obvious, for example, energy spectra become discrete. Of particular interest is the class of devices that are composed of combinations of lattice mismatched materials. These material combinations, such as Si_xGe_{1-x}/Si and $In_xGa_{1-x}As$/GaAs are selected primarily on the basis of their electronic properties and to some extent for convenience of processing. Usually, the QD is buried in the host matrix with differing elastic constants and lattice parameter. Because of the lattice mismatch, both the QD and host matrix strain and relax elastically to accommodate this mismatch and thus admit a state of stress. As is well known, the electronic structure and the consequent optoelectronic properties of QDs are severely impacted due to this lattice mismatch induced strain. The host matrix boundaries do not impact its strain state, if the distance of the QD from any free boundary is significantly larger than e.g. the QD radius (typically $> 3R$).

The conductivity of the semiconductors can be represented by the energy band of semiconductors. Since the electronic properties of a semiconductor are dominated by the highest partially empty band and the lowest partially filled band, it is often sufficient to only consider those bands. By adopting this continuum view of confinement in semiconductor quantum devices, the spectrum of confined states available to individual electrons or holes can be characterized by the steady state Schrodinger equation, given by:

$$H_{\alpha\beta}(\vec{\mathbf{r}})\psi_{\beta}(\vec{\mathbf{r}}) + V_{\alpha\beta}(\vec{\mathbf{r}})\psi_{\beta}(\vec{\mathbf{r}}) = \lambda_{\mathrm{E}}\psi_{\alpha}(\vec{\mathbf{r}}). \qquad (2)$$

The form of the Hamiltonian function is directly associated with the type of semiconductors, and especially with the form of the energy band. In view of that, we introduce the following division:

1. One band envelope-function formalism for electrons and holes in which the effective Hamiltonian is given by:

$$H_{\alpha\alpha} = -div\left(\frac{\hbar^2}{2m_{\alpha}(\lambda_E)} grad\psi_{\alpha}\right), \quad \alpha = i = 1,2, \quad (3)$$

where the index i corresponds to the quantum dot ($i = 1$) and to the matrix ($i = 2$), respectively Such a description is valid for the direct band gap and for instance is valid for an InAs quantum dot embedded in a GaAs matrix. In the present analysis the electron effective mass m_i is assumed to be constant on the quantum dot and the matrix for every fixed energy level λ_{E} and is taken as [12]:

$$\frac{1}{m_i(\lambda_E)} = \frac{P_i^2}{\hbar^2}\left(\frac{2}{\lambda_E + E_{g,i} - V_i} + \frac{1}{\lambda_E + E_{g,i} - V_i + \delta_i}\right), \quad (4)$$

where the confinement potential V_i is piecewise constant, and P_i, $E_{g,i}$ and δ_i are the momentum matrix element, the band gap, and the spin-orbit splitting in the valence band for the quantum dot (i=1) and the matrix ($i = 2$), respectively. The values of the above constants are given in Table 1.

Table 1
The material properties of the quantum dot InAs and the matrix GaAs

	P_i	$E_{g,i}$	V_i	δ_i
i=1 (QD) InAs	0.8503	0.42	0	0.48
i=2 (matrix) GaAs	0.8878	1.52	0.7	0.34

2. The highest energy valence subbands. This basis consists of the two degenerate heavy hole subbands and the two degenerate light hole subbands, in reference to the relative masses of the charge carriers when treated as classical particles. The form of the Hamiltonian is given by:

$$H_{\alpha\beta} = -\frac{\hbar^2}{2m_0} L^{kl}_{\alpha\beta}(\vec{\mathbf{r}})\nabla^2_{kl}, \quad \alpha,\beta,k,l = 1,2, \qquad (5)$$

where

$$L^{kl}_{\alpha\beta}(\vec{\mathbf{r}}) = \begin{bmatrix} \mathrm{g}_1^{\mathrm{kl}} & \mathrm{g}_2^{\mathrm{kl}} & \mathrm{g}_3^{\mathrm{kl}} \\ \mathrm{g}_2^{\mathrm{kl}} & \mathrm{g}_4^{\mathrm{kl}} & \mathrm{g}_5^{\mathrm{kl}} \\ \mathrm{g}_3^{\mathrm{kl}} & \mathrm{g}_5^{\mathrm{kl}} & \mathrm{g}_6^{\mathrm{kl}} \end{bmatrix}. \qquad (6)$$

This Hamiltonian can be used to model the medium in a Si_xGe_{1-x} structure. g_1, g_2, and g_3 are the Luttinger-Kohn parameters – see Singh [13, 14].

3. A model for spin-dependent transport in the quantum dot regime of a carbon nanotube is much more complicated as it may be seen e.g. in Ref. [15]. Those problems are not discussed herein.

The nonuniform potential field V in Eq. (2) includes all energetic effects on the charge carrier due to sources other than the background periodic crystalline potential. The effects to be considered include the relative offset of the valence band in adjacent layers of the heterostructure, and the effect of the elastic strain field. The potential field can be written as the sum of these two contributions, so that:

$$V_{\alpha\beta}(\vec{\mathbf{r}}) = V_{\alpha\beta band}(\vec{\mathbf{r}}) + V_{\alpha\beta strain}(\vec{\mathbf{r}}). \qquad (7)$$

The first term in Eq. (7) depends on the form of the semiconductor and is defined by the material constants in the similar manner as presented in Table 1.

Elastic strain in the structure induces a potential that shifts and couples the energy bands in the crystal. Based on deformation potential theory, the calculated strain tensor $\varepsilon^{ij}(\vec{\mathbf{r}})$ can be used to generate a potential by means of the operation:

$$V_{\alpha\beta strain}(\vec{\mathbf{r}}) = D^{\xi\eta}_{\alpha\beta}\varepsilon^{\xi\eta}(\vec{\mathbf{r}}). \qquad (8)$$

The form of $D^{\xi\eta}_{\alpha\beta}$ is similar to the form of $L^{\xi\eta}_{\alpha\beta}$ given in Eq. (6) or may be determined with the use of the classical Eshelby method.

It is worth to mention herein that the relation (8) can be introduced also in the nonlinear form as proposed e.g. by

Melnik, Mahapatra [16]. The authors analysed also the influence of the electromechanical effects on the eigenenergies of semiconductors.

The weak form of the equation (2) is obtained by forming the inner product of each term in the equation with the wave function vector field ψ_β and integrating over the volume of the body. Multiplying (2) by ψ_α in the Sobolev space $H_1^0(\Omega)$ by parts one gets the variational form of the Schrödinger equation:

$$\int_\Omega \left(\psi_\alpha(\vec{\mathbf{r}})\, H_{\alpha\beta}(\vec{\mathbf{r}})\, \psi_\beta(\vec{\mathbf{r}}) + \psi_\alpha(\vec{\mathbf{r}})\, V_{\alpha\beta}(\vec{\mathbf{r}})\, \psi_\beta(\vec{\mathbf{r}})\right) d\Omega = \lambda_E \int_\Omega \psi_\alpha(\vec{\mathbf{r}})\, \psi_\beta(\vec{\mathbf{r}})\, d\Omega. \tag{9}$$

Equation (2) is the Euler equation which results from the requirement that Eq. (9) must be stationary under variations in ψ_α. Finally, the solution can be found using the classical Rayleigh functional. The evaluation of the nonlinear Rayleigh functional is based on the discretization method of the eigenvectors ψ_α. For one band Hamiltonian (3) the problem (9) is reduced to the nonlinear eigenvalue problem, whereas for Hamiltonian defined by Eq. (5) leads to the linear one.

Many of the previous numerical modeling approaches for these quantum structures used spatial discretization methods, such as the finite element or finite difference method [17–19]. As an alternative, the boundary element method was proposed by Geldbard, Malloy [20]. Voss [21] employed the Rayleigh-Ritz method to solve the nonlinear eigenvalue problem where the eigenstates of the electron in QDs were derived with the use of the finite element method incorporated in the MATLAB package. Wavelet bases appear to be attractive as a general approach for a wide range of potentials, and not only for quantum dots. In the mathematical sense the problem is described by the solution of the Helmholtz equation. Various aspects of the evaluation of the eigenenergies in closed periodic systems of quantum dots were also discussed in the literature – see e.g. Ref [22].

3. Carbon nanotubes

Buckling, free vibrations or structural instability form a fundamental consideration in the mechanics of carbon nanotubes (CNTs) due to the slender and thin walled nature of their structure. In the last two decades, intensive studies have been performed to achieve an in-depth understanding on this issue [23, 24]. As reviewed in Ref [23], such an investigation was first focused on the fundamental buckling case of CNTs. The effect of the interlayer van der Waals (vdW) interaction is a major issue for the buckling of multiwalled CNTs (MWCNTs). The Whitney–Riley model may be used to determine a spring constant characterizing vdW interaction [25]. It is observed that the effect of matrix on the radial vibration frequencies/buckling loads of MWNTs is dependent on the stiffness of matrix and the innermost diameter of MWNTs.

The buckling/free vibrations are usually investigated with the help of three different analytical and numerical models:

- the continuous orthotropic cylindrical shell model,
- the Euler beam model and
- the molecular dynamic model based on the interatomic interactions potentials.

As usual, buckling/free vibrations of a structure is referred as the change of its equilibrium state from one configuration to another at a critical, usually, compressive load. For linear problems the analysis can be reduced to the following eigenvalue problem:

$$\left(K_{\alpha\beta} + \lambda_b K_{g\alpha\beta}\right) q_\alpha = \{\mathbf{0}\}, \tag{10}$$

where $\{\mathbf{0}\}$ denotes the zero matrix. We do not intend to dwell on the strict definition of their forms because it is given in the explicit form, and, on the other hand, their form is directly connected with the form of the laminated structure (beams, plates, cylindrical panels). The form is directly equivalent to the eigenproblem (1).

3.1. Shell/beam model. An explicit expression for the critical buckling strain/free vibrations can be derived based on cylindrical shell models. However, in the literature it is demonstrated that for small radius of the nanotubes the buckling mode falls into the regime of Euler beam buckling (R<0.8 [nm]) and then with the increase of the radius the circumferential modes of buckling (i.e. for n>1) becomes to be dominant. Therefore the analytical studies are limited to the axisymmetric buckling/vibration analysis only, i.e. n=0 and m>0. For simply supported cylindrical shells made of a specially orthotropic material the eigenfrequencies can be easily derived in the analytical way using the Rayleigh-Ritz method as the roots of the following equation:

$$\chi_b^3 + b_0\chi_b^2 + c_0\chi_b - d_0 = 0, \tag{11}$$

where

$$\begin{gathered} b_0 = -a_{11} - a_{22} - a_{33}, \\ c_0 = a_{11}a_{22} + a_{11}a_{33} + a_{22}a_{33} - a_{13}^2, \\ d_0 = a_{11}a_{22}a_{33} - a_{22}a_{13}^2, \qquad a_{11} = \zeta_m^2, \\ a_{22} = \frac{A_{66}}{A_{11}}\zeta_m^2, \qquad a_{33} = \frac{A_{22}}{A_{11}} + \frac{h^2}{12R^2}\zeta_m^4, \\ a_{13} = -\frac{A_{12}}{A_{11}}\zeta_m, \qquad \zeta_m = \frac{m\pi R}{L}, \\ \chi_b = \rho R^2 h\omega^2/A_{11}. \end{gathered} \tag{12}$$

The roots of Eq. (2) can be represented as follows:

$$\begin{gathered} \chi_{b1} = a_{22}, \\ \chi_{b2,3} = \frac{1}{2}\left(a_{11} + a_{33} \pm \sqrt{a_{11}^2 + 4a_{13}^2 - 2a_{11}a_{33} + a_{33}^2}\right). \end{gathered} \tag{13}$$

If the carbon nanotube arrays are assumed to be transversely isotropic the material properties in the circumferential and thickness directions are identical. However, the twisted array SWCN is a helical array then, in fact, the nanotube does not possesses completely transversely isotropic properties. Therefore five material constants are necessary to characterize the CNT array behavior. The values of constants take the following form: $E_1 = 580$ [GPa], $E_2 = E_3 = 9.4$ [GPa],

$\nu_{12} = \nu_{13} = 0.18$, $\nu_{23} = 0.90$, $G_{12} = G_{13} = 17.2$ [GPa], $G_{23} = 2.47$ [GPa]. In addition let us assume $\rho = 600$ [kg/m^3] and $L = 29.5$ [nm].

Thus, for $\chi_b = 1$ the square root of the ratio $A_{11}/(\rho h R^2)$ is equal to 6.55 [THz] (n1 = n2 = 5) and is the multiplier of natural frequencies – Eq. (3). As it may be seen the magnitude of natural frequencies (THz) is in the range mentioned in the literature. For (n1 = 5, n2 = 5) carbon nanotubes the radius R = 0.339 [nm] the parameter $\zeta_m = 0.0314^*$m and it is treated as negligibly small. Since all membrane stiffnesses A_{ii} are proportional to the thickness parameter h so that that constant can be omitted in the further considerations. Figure 1 demonstrates the comparison of the values of the frequencies described by Eqs. (12) and the value corresponding to the Euler beam model which is given by the relation:

$$\chi_{bEuler} = \left(m\pi\frac{h}{L}\right)^2 \zeta_m^2. \tag{14}$$

In Fig. 1 the x-axis corresponds to the value ζ_m^2 and the y-axis represents the value χ_b/ζ_m^2. As it may be easily noticed from the relations (11) the first shell mode is constant and equal to a_{22}/ζ_m^2, the second – a_{33}/ζ_m^2 and the third (not plotted in Fig. 1) is equal to a_{11}/ζ_m^2 so that is equal to 1. It is necessary to emphasize that the above formulas are the approximations only for the second and the third modes but they are satisfactory for the present numerical data. In the second shell mode and in the Euler beam model the shell thickness h is equal to 0.34 [nm]. In the plot the first shell mode corresponds to the lowest frequency. It is worth to mention also that in the literature the frequencies are usually compared with values obtained with the use of the Euler beam model. However, the use of the shell model allows us to predict lower value but the relation between those values is strongly dependent on the assumed CNT length L. For higher values the Euler value can be lower than that corresponding to the application of the shell model.

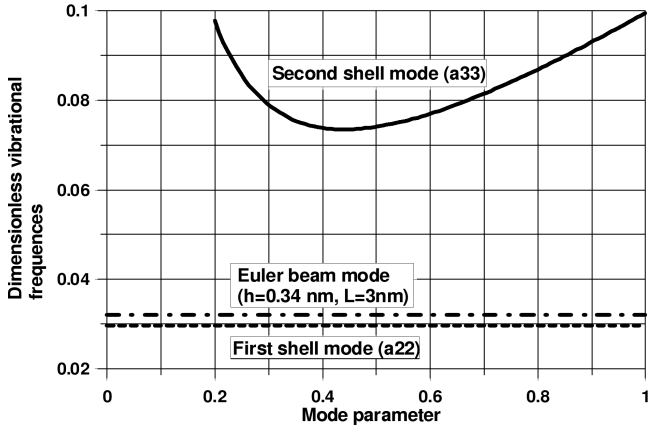

Fig. 1. Comparison of vibrational frequencies for different models

Continuum cylindrical shell models have been widely applied in the buckling/free vibration analysis of carbon nanotubes. Using the cylindrical models it is possible to evaluate buckling loads/free vibrations of cylindrical shells, analyze their post-buckling behaviour etc. employing the methods of analysis well-known for eigenvalue shell problems. In this way it is possible to describe the behaviour of equivalent carbon single-walled or multi-walled carbon nanotubes. However, there is always an open question dealing with the accuracy and correctness of such approaches.

Peng et al. [26] determined the order of error for approximating the single-walled carbon nanotubes by a thin shell. The ratio of atomic spacing r_0 to the single-walled carbon nanotubes radius R, is used to identify the order of error. They considered the structural response of the single-walled carbon nanotubes subject to tension (or compression), torsion, bending and internal (or external) pressure. They proved that only for the order of error equal to 40% – (5,5) armchair single walled carbon nanotubes can be modeled as thin shell with a constant thickness and isotropic mechanical properties.

The extensions of the above results have been presented by Wu et al. [27]. The authors have defined the degrees of: anisotropy, nonlinearity and coupling, i.e., down to what single-walled carbon nanotubes radius the tension/bending coupling becomes negligible in the constitutive relations.

Numerical modeling of single-walled carbon nanotubes constitutes the separate class of problems. Some of them are discussed by Kalmakarov et al. [28]. The cited work presents also the comparison of Young's modulus and the equivalent thickness predicted with the use of various theories.

The broader discussion of those problems can be found in Ref. [29]. Muc et al. [11, 30] demonstrated also the effectiveness of the shell models in the identification of defects occurring in the CNTs.

3.2. Molecular dynamic model. Let us consider that the hexagon, which is the constitutional element of CNTs nanostructure, is simulated as structural element of a space-frame made of 3D beams. Of course, in the same way the entire nanotube lattice may be modelled. The simulation leads to the correspondence of the bond length C-C with the 3D beam element length L and with the element diameter d characterizing a circular cross-sectional area for the element. The linkage between molecular and continuum mechanics can be made by an appropriate definition of 3D beam mechanical properties.

Based on the energy equivalence between local potential energies in computational chemistry and elemental strain energies in structural mechanics, we can determine the tensile resistance, the flexural rigidity and the torsional stiffness for an equivalent beam. If the beam element is assumed to be of round section, then only three stiffness parameters, i.e., the tensile resistance EA, the flexural rigidity EI and the torsional stiffness GJ, need to be determined for deformation analysis. By considering the energy equivalence, a direct relationship between the structural mechanics parameters and the molecular mechanics force field constants can be established:

$$\frac{E_i A_i}{l_i} = k_{ri}, \qquad \frac{E_i I_i}{l_i} = k_{\theta i}, \qquad \frac{G_i J_i}{l_i} = k_{ti}, \tag{15}$$

where k_{ri}, $k_{\theta i}$ and k_{ti} are the force field constants in molecular mechanics. They are indexed by the number of the beam

occurring in the RVE for a given nanotube structure. For zigzag and armchair configurations the RVE are plotted in Fig. 2.

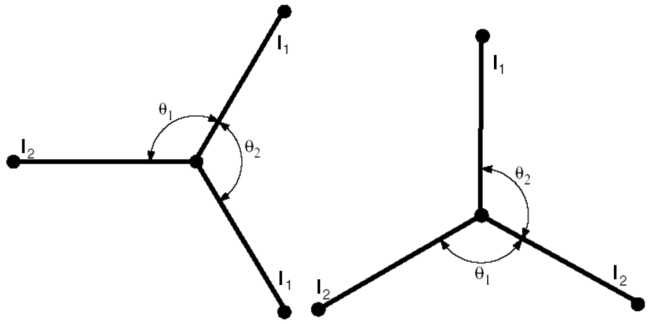

Fig. 2. Representative volume elements of an a) armchair CNT and b) zigzag CNT

Let us note that the present formulation incorporates special features of molecular mechanics models. In addition, it allows to analyze large deformations of CNTs since the beam length L in Eq. (14) is replaced by an actual beam length l_i different for different i-th beams in the RVE.

By comparing energies of the mechanical and molecular diatomic systems the force constants k_{ri}, $k_{\theta i}$ can be derived. Using the interatomic potentials, the stretching force that results from the bond elongation Δl_i and the twisting moment that results from the bond angle variation $\Delta\theta_i$ can be calculated as follows:

$$F(\Delta l_i) = \frac{\partial V}{\partial l_i}, \qquad M(\Delta\theta_i) = \frac{\partial V}{\partial \theta_i}, \qquad \Delta l_i = l_i - l_{0i}, \qquad \Delta\theta_i = \theta_i - \theta_{0i}, \qquad i = 1, 2. \tag{16}$$

The derivatives in Eq. (15) are expanded in the Taylor series up to the first derivative (linear terms) only. However, the initial values r_{0i} and θ_{0i} are modified at each iteration step since, in fact, both the stretching forces and the twisting moments are nonlinear with respect to the bond length and to the bond angle, respectively.

By assuming a circular beam section with diameter d_i, and setting $A_i = \pi d^2/4$, $I_i = \pi d^4/64$, Eqs. (14,15) give:

$$d_i = 4\sqrt{\frac{k_{\theta i}}{k_{ri}}}, \qquad E_i = \frac{k_{ri}^2 l_i}{4\pi k_{\theta i}}. \tag{17}$$

Then, following the procedure of the finite element structural mechanics technique, the nanotube deformation under certain loading conditions can be readily solved. It is worth to note that Young's moduli E_1 and E_2 are different even for the linear part of the stress-strain curve since the beam lengths r_i are different at each iteration step, and the force constants k_{ri} and $k_{\theta i}$ are nonlinear functions of r and θ, respectively, as the second derivatives of the interatomic potential.

The numerical space-frame model of carbon nanotubes is presented in Fig.3. One of the ends of the tube is simply supported, whereas at the second the symmetry conditions are imposed. The carbon nanotubes remain cylindrical until the critical eigenfrequency is reached at which point they deform in the longitudinal direction (i.e. $n = 0$). The half of nanotubes is modeled only due to symmetric boundary conditions. The natural frequencies have been obtained with the use of the NISA FE package.

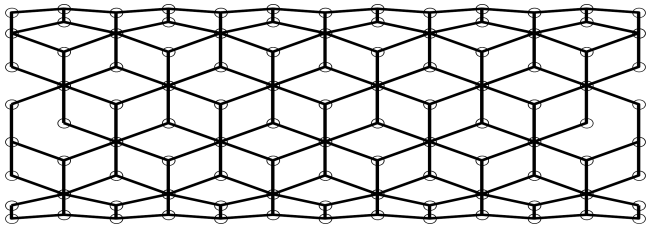

Fig. 3. Numerical space-frame model of the (5,5) carbon nanotube

The carbon nanotubes remain cylindrical until the critical eigenfrequency is reached at which point they deform in the longitudinal direction. Figure 4 is a plot of some typical modes of deformations for the first natural frequency The magnitude of natural frequencies (THz) is in the range mentioned in the literature.

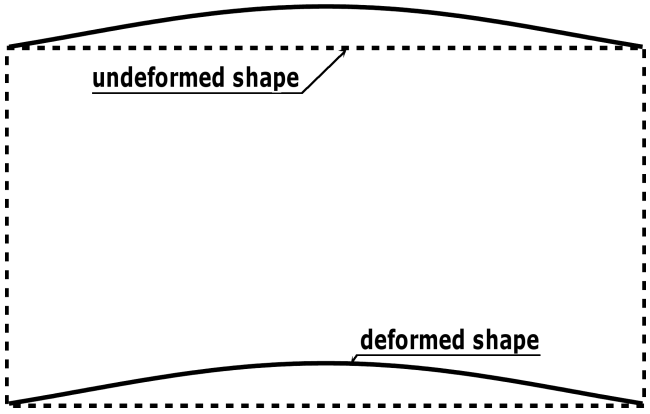

Fig. 4. Mode I – frequency = 3.472 THz (deformations not to scale)

3.3. Quantum mechanics. The quantum mechanics approach is an approximate solution of the Schrodinger-like equation. The analysis starts from solving the one-electron Schrödinger equation in the form given by Eq. (2) where $\alpha = \beta = 1$. This equation is solved with the ansatz that the single electron states can be represented in terms of atomic orbitals located on each single atom. The number of atomic orbitals n is usually taken equal with the number of valence electrons for the atomic species (for example $n = 4$ for carbon). Let N_t (usually a large number) the number of translational cells (for instance in the form presented in Fig. 2) over which periodic boundary condition are imposed and let N be the number of atoms in each cell. If no explicit recourse to translational symmetry is made, the one-electron eigenfunctions ψ are represented in terms of localized orbitals functions and expansion coefficients. The expansion coefficients grouped in the vector should be obtained from the one-electron generalized $N \times N$ ($N = nN_tN$) eigenvalue problem. which can be easily obtained by substituting the one-electron eigenfunctions ψ are representations (in terms of localized orbitals functions and expansion coefficients) into Eq. (2) that finally forms the matrix form of the

Schrödinger equation. In such an equation (the NxN eigenvalue problem) the N electronic state levels appear. It cannot be solved directly. The usual approach is to introduce a significant computational simplification by explicitly accounting for the translational symmetry. For large N it leads to dense solutions of large sparse problems. The number of states corresponds directly to the length of nanotubes. For such a class of eigenproblems Lanczos shift-and-invert method is preferred in most practical cases. In addition, clustering eigenvalues are transformed to well-separated eigenvalues. In this way it is possible to find more energetically favorable nanostructures and therefore more likely to be stable.

4. Concluding remarks

In this contribution, we analyzed fundamental approaches in bridging the scales in mathematical models for the description of various problems encountered in nanomechanics, especially for such nanostructures as quantum dots and carbon nanotubes. We demonstrated that the variety of eigenproblems well-known in the classical mathematics for computing the energy levels and the wave functions can be easily adopted in solving different problems existing in the analysis of nanostructures behaviour.

However, several avenues of research remain open and inadequately addressed. We highlight some of our own personal perspectives here. More information about those problems can be found e.g. in Refs. [31, 32].

REFERENCES

[1] R. Courant and D. Hilbert, *Methods of Mathematical Physics*, John Wiley & Sons, London, 2008.

[2] An H. Lę, *Nonlinear Eigenvalue Problems*, Department of Mathematics, University of Utah, Salt Lake City, 2005.

[3] G. Prodi, *Eigenvalues of Non-Linear Problems*, Springer, Berlin, 2010.

[4] V. Mehrmann and H. Voss, "Nonlinear eigenvalue problems: a challenge for modern eigenvalue methods", *GAMM Mitteilungen* 28, CD-ROM (2005).

[5] V. Mehrmann and D. Watkins, *Polynomial Eigenvalue Problems with Hamiltonian Structure*, ETNA, London, 2002.

[6] R.H. Baughman, A.A. Zakhidov, and W.A.D. Heer, "Carbon nanotubes-the route toward applications", *Science* 297, 787–792 (2002).

[7] D. Srivastava, C. Wei, and K. Cho, "Nanomechanics of carbon nanotubes and composites", *Applied Mechanics Reviews* 56, 215–230 (2003).

[8] P. Ajayan and T. Ebbesen, "Nanometre-size tubes of carbon", *Reports on Progress in Physics* 60, 1025–1062 (1997).

[9] C. Dekker, "Carbon nanotubes as molecular quantum wires", *Physics Today* 52, 22–28 (1999).

[10] P. Harris, *Carbon Nanotubes and Related Structures: New Materials for the 21st Century*, Cambridge University Press, Cambridge, 1999.

[11] A. Banaś and A. Muc, "Current problems in design of quantum dots used in semiconductors", *Key Eng Mat.* 542, 1–6 (2013).

[12] A. Zaslavsky, K.R. Milkove, Y.H. Lee, B. Ferland, and T.O. Sedgewick, "Strain relaxation in silicon/germanium microstructures observed by resonant tunneling spectroscopy", *Applied Physics Letters* 67, 3921–29 (1995).

[13] J. Singh, *Physics of Semiconductors and Their Heterostructures* McGraw-Hill, New York, 1993.

[14] B. Lassen, L.C.L.Y. Voon, M. Willatzen, and R.V.N. Melnik "Exact envelopefunction theory versus symmetrized Hamiltonian for quantum wires: a comparison", *Solid State Commun* 132, 141–149 (2004).

[15] S. Koller, L. Mayrhofer, and M. Grifoni, "Spin transport across carbon nanotube quantum dots", *New Journal of Physics* 9, 348–384 (2007).

[16] R. Melnik and R. Mahapatra, "Coupled effects in quantum dot nanostructures with nonlinear strain and bridging modelling scales", *Computers and Structures* 85, 698–711 (2007).

[17] M. Grundmann, O. Stier, and D. Bimberg, "InAs/GaAs pyramidal quantum dots: Strain distribution, optical phonons, and electronic structure", *Phys. Rev.* B 52, 11969–11981 (1995).

[18] O. Stier, M. Grundmann, and D. Bimberg, "Electronic and optical properties of strained quantum dots modeled by 8-band k·p theory", *Phys. Rev.* B 59, 5688–5701 (1999).

[19] H.T. Johnson and L.B. Freund, The influence of strain on confined electronic states in semiconductor quantum structures, *Int. J. Sol. Struct.* 38, 1045–1062 (2001).

[20] F. Gelbard and K.J. Malloy, "Modeling quantum structures with the boundary element method", *J. Comp. Phys.* 172, 19–39 (2001).

[21] H. Voss, "Numerical calculation of the electronic structure for three-dimensional quantum dots", *Comp. Phys. Communications* 174, 441–446 (2006).

[22] A. Muc, A. Banaś, and P. Kędziora, "An analytical solution for conical quantum dots", *J. Th. Appl. Mech.* 51, 387–392 (2013).

[23] C.Y. Wang, Y.Y. Zhang, C.M. Wang, and V.B.C. Tan, *J. Nanosci. Nanotechnol*. 7, 4221 (2007).

[24] A. Muc, "Design and identification methods of effective mechanical properties for carbon nanotubes", *Mat&Design* 31, 1671–1675 (2010).

[25] V.Z. Vlasov and U.N. Leont'ev "Beams, plates and shells on elastic foundations", *Israel Program for Scientific Translations*, Jerusalem, 1966.

[26] J. Peng, J. Wu, K.C. Hwang, J. Song, and Y. Huang, "Can a single-wall carbon nanotube be modeled as a thin shell?", *J. Mechanics and Physics of Solids* 56, 2213–2224 (2008).

[27] J. Wu, J. Peng, K.C. Hwang, J. Song, and Y. Huang, "The intrinsic stiffness of single-wall carbon nanotubes", *Mechanics Research Communications* 35, 2–9 (2008).

[28] A. Kalamkarov, A. Georgiades, S. Rokkam, V. Veedu, and M. Ghasemi-Nejhad, "Analytical and numerical techniques to predict carbon nanotubes properties", *Int. J. Solids and Structures* 43, 6832–6854 (2006).

[29] A. Muc, "Modelling of carbon nanotubes behaviour with the use of a thin shell theory", *J. Th. Appl. Mech.* 49, 531–540 (2011).

[30] A. Muc and M. Chwał, "Vibration control of defects in carbon nanotubes", *Solid Mechanics and Its Applications* 30, 239–46 (2011).

[31] G. Szefer and D. Jasińska, "Modeling of strains and stresses of material nanostructures", *Bull Pol. Ac.: Tech* 57, 41–46 (2009).

[32] P. Martyniuk and A. Rogalski, "Insight into performance of quantum dot infrared photodetectors", *Bull. Pol. Ac.: Tech.* 57, 103–116 (2009).